CAMERA ARTIFACTS IN IUE LOW-DISPERSION SPECTRA

D. Michael Crenshaw[1], Otto W. Bruegman[2],

and Dara J. Norman[1]

To appear in the April, 1990 issue of

the *Publications of the Astronomical Society of the Pacific*

[1] Astronomy Programs, Computer Sciences Corporation

[2] Computer Technology Associates, Inc.

ABSTRACT

Sky background images obtained by the International Ultraviolet Explorer (IUE) were analyzed to study artificial spectral features (camera artifacts) in low-dispersion spectra. The artifacts mimic emission features, and have been present in long-exposure spectra since launch of the IUE satellite. The camera artifacts are strong in spectra characterized by long exposure times because they scale in time-integrated flux with the background level, which increases during the exposure due to camera phosphorescence. The artifacts cannot be detected in spectra obtained from short, direct exposures of flat-field lamps or standard stars. Plots of average sky background spectra for the three operational IUE cameras (SWP, LWP, and LWR) are given to aid scientists in the identification of artifacts in their spectra.

I. Introduction

The International Ultraviolet Explorer (IUE), launched on 1978 January 26, has provided ultraviolet spectra of astronomical objects for over a decade. The stability and endurance of the IUE spectrograph cameras have been major factors in the establishment of this enormously useful data base. The IUE cameras are SEC Vidicons coupled to ultraviolet-to-visible image converters (UVC) and have a limited dynamic range: each pixel in a raw image can have a value from 0 to 255 data numbers (DN). Prior to each exposure, a reproducible pedestal of 15 to 40 DN is placed on the image by exposing to a tungsten flood (TFLOOD) lamp, reading the camera with a defocused beam, and exposing and reading again. As a result of repeated exposures, the phosphor target in the UVC glows at a rate that ranges from 5 to 10 DN per hour per pixel (Grady and Imhoff 1985). The IUE cameras record spectra in two wavelength regions: the SWP camera obtains spectra in the approximate range 1150 to 2000 Å , and the LWP and LWR cameras obtain spectra in the approximate range 1800 to 3200 Å . Spectra can be obtained for each wavelength region in either low-dispersion (R = 200 to 400) or high-dispersion (R = 12,000) mode (for more details see Boggess et al. 1978).

The existence of artificial spectral features in low-dispersion IUE spectra has been known for some time. Obvious sources of artificial features are cosmic-ray hits, hot pixels, and the reseaux etched on the faceplates of the cameras (Grady and Imhoff 1985). The reseaux and hot pixels occur at relatively fixed locations on raw IUE images, and are flagged by the IUE Spectral Image Processing System (IUESIPS). The cosmic-ray hits in the background region can by detected by inspection of the raw images; hits in the spectral region can be detected by comparing more than one image of the same target. A more insidious source of confusion is the "fixed-pattern" found in both low- and high-dispersion spectra with a wide range of exposure times (Hackney, Hackney, and Kondo 1984; Adelman and Leckrone 1985). Much of the fixed-pattern is probably due to misalignment of the science image with the ITF images used to flat-field the science image (Linde and Dravins 1988; Nichols-Bohlin 1988).

This paper presents a detailed study of another source of artificial features, labeled "camera artifacts" by the first investigators to study them in detail (Hackney, Hackney, and Kondo 1984, 1985). These investigators found that artificial emission features appear at fixed locations in SWP spectra with long exposure times, but are not detectable in SWP spectra with exposure times less than about an hour. The artifacts could potentially be the source of much confusion for scientists, since they appear on every long exposure of a target and are therefore not caused by one-time events such as cosmic-ray hits. As part of a massive effort by the IUE project to investigate means to improve the signal-to-noise ratio, resolution, photometric accuracy, and wavelength calibration of IUE data, a detailed study of camera artifacts was initiated. This paper deals with the appearance of these features in low-dispersion IUE spectra; artifacts in high-dispersion spectra have not yet been studied. A preliminary report on our study of SWP camera artifacts was published in an IUE Newsletter (Bruegman and Crenshaw 1989). In this paper we give new results for the LWP and LWR cameras and a comprehensive analysis for the SWP camera, which has the most pronounced artifacts.

The best way to study camera artifacts is to obtain sky background images with a large range in exposure times, since any artifacts seen in a given sky background spectrum will also be present in a spectrum of an astronomical target with a similar exposure time. It will be demonstrated that only one feature seen in a sky background spectrum is due to real sky emission: the well-known line of geocoronal Lα. Other strong features are artificial, and can be studied best in images that lack the confusing presence of a "real" spectrum.

II. Observations and Data Reduction

Most of the sky background images were obtained by the IUE observatory staff specifically for this study. IUE has a large aperture (10″x 20″oval) for each wavelength region (one for the SWP and one for the LWP or LWR), and the capability to expose more than one camera at a time. The standard procedure for obtaining these observations is to begin an exposure in one wavelength region on a guest observer's target, then start an exposure on the sky in the other wavelength region, and finally read the sky background exposure before the first exposure is finished. The sky backgrounds are therefore obtained at no cost in observing time to the guest observer. The large apertures are separated by 66 ″(see Sonneborn et al. 1987 for a detailed diagram of the aperture plate), so sky backgrounds were not taken when the telescope was pointed at an extended source or a crowded star field. Some sky background spectra, particularly the short-exposure ones, have been obtained by guest observers for their own purposes; these were retrieved from the IUE archives for this study.

To identify all of the useful data, the IUE Merged Log was searched for all images with an object classification code of 7, which designates interplanetary medium or sky background exposures, and with exposure times greater than or equal to 30 minutes. The photowrites of the raw images and plots of the reduced spectra were visually inspected, and images with residual spectra from previous overexposures or large cosmic-ray hits in the low-dispersion extraction region were excluded from this study. Tables I, II, and III list the 119 SWP, 46 LWP, and 91 LWR sky background images used for this study. Also listed are the dispersion mode at the time of observation, the exposure time in minutes and seconds, and the processing date specified as the year and day of year.

Although the sky background images used for this study were taken in low- or high-dispersion mode, all were processed by IUESIPS as low-dispersion, large-aperture spectra (see Turnrose and Thompson 1984 for more details on IUESIPS processing). Each image was processed to yield a line-by-line, spatially-resolved (LBLS) file, which represents a series of spectra in the spatial direction. All subsequent reductions and analyses were performed by the authors at the Goddard Regional Data Analysis Facility (RDAF) using standard RDAF software. With the same parameters as those used by IUESIPS, the lines in each LBLS file were coadded in the spatial direction to obtain two merged spectra: a point-source (9 lines) and an extended-source (15 lines) spectrum. The May 1980 absolute calibration curves (Bohlin et al. 1980) were used to obtain merged spectra in units of time-integrated flux (ergs cm^{-2} $Å^{-1}$) as a function of wavelength (Å). To compare with the units used by most guest observers, the spectra were also divided by the exposure time to obtain flux (ergs sec^{-1} cm^{-2} $Å^{-1}$) as a function of wavelength (Å).

Since an individual sky backbround spectrum is rather noisy, the spectra were separated into groups and averaged. The averages were computed so that spectra with bad quality data (due to a reseau, microphonic noise, telemetry dropout, hot spot, etc.) at a particular wavelength were not included in the average at that wavelength. In general, ten or more spectra were included in any average to reduce the chance that a weak cosmic-ray hit not flagged by IUESIPS would result in a significant feature in the average spectrum. Unless otherwise stated, the average spectra were computed from subsets of all sky background images with exposure times between 180 and 440 minutes which were processed with the "new" IUESIPS software (implemented at Goddard on November 10, 1981 and at VILSPA on March 11, 1982). The old processing software used very different methods of geometric and photometric correction (Turnrose, Harvel, and Stone 1981; Turnrose and Thompson 1984). The restrictions on exposure times were imposed when it was desirable to reduce exposure time effects.

In order to compare the sky backgrounds with direct flat-field exposures, a sequence of TFLOOD exposures was obtained for each camera; each TFLOOD image was obtained by directly exposing the camera to a tungsten flood-lamp. Table IV lists the 18 SWP, 16 LWP, and 12 LWR TFLOOD images obtained. The columns in Table IV give the range in image numbers, the dispersion mode at the time of observation, the exposure time in minutes and seconds, and the year and day of observation. The TFLOOD images have an average exposure level of about 100 DN in the low-dispersion extraction region, which is about the same level that is obtained with a seven-hour sky background exposure. The TFLOOD images were processed and reduced in the exact same manner as the sky background images to yield average point-source and extended-source spectra.

III. Results

a) Characteristics of Camera Artifacts

To verify that the SWP features are actually artifacts, the images processed with the new software and with exposure times between 180 and 440 minutes were divided into two groups: those taken in high-dispersion mode and those taken in low-dispersion mode. Figure 1 shows the average low-dispersion spectra extracted from images obtained in both dispersion modes; point- and extended-source versions are given. If a feature is actually due to sky emission, then it will appear at a different pixel location in low-dispersion images than in high-dispersion images. Thus, real sky features seen in low-dispersion spectra extracted from low-dispersion images will not be seen in low-dispersion spectra extracted from high-dispersion images. It is clear from Figure 1 that, with the obvious exception of geocoronal $L\alpha$ at 1216Å , the strong features in the low-dispersion average are also present in the high-dispersion average. Thus there is no evidence for real sky features other than geocoronal $L\alpha$.

Also plotted in Figure 1 is the average of the SWP TFLOOD spectra. Although the exposure levels (in DN) for sky background and TFLOOD spectra are about the same, the strong artifacts seen in the sky backgrounds are not present in the TFLOODS. Examination of IUE standard star spectra with exposure times on the order of minutes or less reveals no evidence for strong artifacts. This confirms the finding by Hackney, Hackney and Kondo (1984, 1985) that these features are not detected in short-exposure spectra.

Another important issue to investigate is the reproducibility of the artifacts over time. The sky background spectra were divided into four chronological groups; each group contains about two years of data. The average spectra for both point- and extended-sources are shown in Figure 2, with the early spectra at the top (note that the earliest spectra were processed with the old software, and are smoother due to the larger wavelength bins). It is clear from a comparison of the strong emission features that the narrow camera artifacts have persisted over the lifetime of IUE. However, the large-scale structure, particularly the bump at 1450-1600 Å , is enhanced at later times. The source of the large-scale structure is unknown and currently under investigation.

The same techniques for studying SWP camera artifacts were used to study artifacts in the LWP and LWR cameras. Figures 3 and 4 show the average spectra in the wavelength region 2400 - 3000 Å for the sky backgrounds and TFLOODS. The sky background spectra extracted from low- and high-dispersion images show similar features; there is no evidence for any real sky emission. The TFLOOD spectra, which are at about the same exposure level as the sky backgrounds, exhibit a fixed-pattern that is not the same as that in the sky backgrounds. It is apparent that the long-wavelength cameras do not exhibit as many high-contrast features as seen in the SWP camera, which may be the reason that no previous identifications of artifacts in LWP and LWR spectra have been published.

b) Effects of Exposure Time

To study the effects of exposure time on the camera artifacts, sky background spectra that were processed with the new software were separated into groups according to exposure time and averaged. As an example, Figure 5 shows an expanded plot of the extended-source SWP spectra in the wavelength region 1600 - 2000 Å ; the average exposure times range from 33 to 768 minutes. Although some of the structure seems to change with exposure time, most of the strong features are reproduced in all of the spectra. It appears that the emission-line artifacts discovered by previous investigators are just the strong peaks in an overall systematic pattern. It is also clear that this pattern grows in time-integrated flux with exposure time. However, as shown in Figure 1, this is not the same pattern seen in short, direct TFLOOD exposures.

To investigate this point further, the time-integrated fluxes of several artifacts were averaged over narrow wavebands that encompass the features to determine their strength (in ergs cm^{-2} Å $^{-1}$). Figure 6 shows the increase in strength with exposure time for artifacts in the spectra of all three cameras, as well as straight-line fits to the data. It appears that the artifacts grow roughly linearly with exposure time, but are at small positive values near zero exposure time. The apparent cause of these non-zero values is the pedestal background level that is placed on the image by the camera preparation sequence before starting the exposure (at zero exposure time, the average background level is 15 to 20 DN for SWP images and 30 to 40 DN for LWP and LWR images). Apparently at exposure times near zero minutes there is already a weak artifact pattern present, although it is probably buried in other types of noise such as random noise, or systematic noise introduced by misregistration with the ITF images.

c) Reference Artifact Spectra

The basic purpose of this paper is to give sky background spectra that can be used as reference spectra by scientists interested in identifying camera artifacts. All of the individual sky background spectra with exposure times between 180 and 440 minutes were therefore converted to flux units (ergs sec^{-1} cm^{-2} Å $^{-1}$) and averaged. The resulting averages for point- and extended-source spectra are shown in Figures 7, 8, and 9 for the SWP, LWP, and LWR cameras respectively. The average exposure times are close to 300 minutes: 314, 311, and 289 minutes for the SWP, LWP, and LWR spectra respectively.

The reference spectra can be used to obtain a direct estimate of the contaminating effects of the camera artifacts on long-exposure science spectra. For spectra with exposure times outside the approximate range 180 to 440 minutes, the effects of the artifacts can be estimated by scaling their time-integrated fluxes by the ratio of the background level of the science image to the background level of a 300 minute sky background image. The artifacts are usually only important sources of contamination at large exposure times, because the ratio of background to net signal is generally much larger in long-exposure images.

In practice, the artifact fluxes in Figures 7, 8, and 9 may be uncertain by as much as a factor of two, since the phosphorescence rate depends on the previous history of exposures and preparation sequences (Grady and Imhoff 1985). In addition, Figure 5 demonstrates that the artifact structure may change somewhat as a function of exposure time. Thus, the reference spectra can be used for comparision with science spectra, but not for accurately subtracting out the artifacts.

Many of the SWP artifacts are high-contrast features, and can seriously affect the study of emission-line objects such as nebulae and active galaxies. In particular there is a strong artifact at the position of O III] λ1663 in the point-source spectrum; this feature is obscured by a reseau in the extended-source spectrum. In addition, the strongest artifact in the extended-source spectrum is at the position of N III] λ1750. The LWP camera artifacts are very broad and low-contrast. It is doubtful that a reliable artifact pattern can be identified at wavelengths shortward of about 2400 Å in LWP spectra; this region is probably dominated by other sources of noise. The LWR sky backgrounds exhibit a couple of very strong, broad artifacts, as well as the well-known hot spot near 2195 Å .

It is clear from Figures 7, 8, and 9 that most of the artifacts appear as "emission features", and that fluxes measured in broad wavebands will be positive. The positive fluxes likely result from the method of IUESIPS processing, which uses broad median filters in extracting the background from regions perpendicular to the spectral dispersion. This problem should be kept in mind by scientists that average over large bandpasses to look for weak signals in IUE spectra.

IV. Summary

It has been shown that artificial emission features in long-exposure, low-dispersion IUE spectra, which have earned the name "camera artifacts", are part of a systematic pattern that has been present since the launch of IUE. The artifacts appear to scale in time-integrated flux with the total background exposure level; however, these features are not evident in short, direct exposures of either flat-field lamps or standard stars. Thus it appears that these features are inherent to backgrounds that are built up over time as a result of camera phosphorescence, and that the pixel-to-pixel variations in sky backgrounds due to camera phosphorescence are not entirely the same as those in direct exposures. In order to quantify the differences, further work should concentrate on a direct comparison of the raw images for sky backgrounds and flat-field exposures (i.e., TFLOODS or the UVFLOODS used to make the ITF's).

The sky background spectra in Figures 7, 8, and 9 can be used to identify the artifacts and estimate their strength. The spectra are available on-line through the IDL procedure ARTIFACT at the Goddard RDAF, or they can be obtained directly from D. M. Crenshaw by electronic mail. This work was supported by NASA contract NAS5-29375 with the Computer Sciences Corporation.

TABLE 1

SWP Sky Background Images

	Image	Dsp	Time MIN:SC	Date YR/DAY
SWP	1644	H	030:00	79/259
SWP	2862	L	752:00	78/316
SWP	3165	L	060:00	78/313
SWP	3217	L	300:00	78/320
SWP	5325	L	340:00	79/147
SWP	7035	L	180:00	79/302
SWP	9293	L	245:00	80/168
SWP	9829	L	395:00	80/233
SWP	10462	L	370:00	80/299
SWP	28542	L	030:00	86/180
SWP	10672	L	200:00	80/330
SWP	10718	L	165:00	80/337
SWP	10796	L	320:00	80/346
SWP	10802	L	360:00	80/347
SWP	10810	L	375:00	80/349
SWP	10828	L	360:00	80/353
SWP	10942	L	465:00	81/003
SWP	10948	L	720:00	81/003
SWP	13334	L	060:00	81/050
SWP	13466	L	790:00	81/072
SWP	13959	L	340:00	81/132
SWP	14075	L	180:00	81/148
SWP	14266	L	120:00	81/168
SWP	14393	L	735:00	81/187
SWP	14408	L	840:00	81/188
SWP	15336	L	390:00	81/301
SWP	15344	L	328:00	81/303
SWP	15581	L	740:00	81/333
SWP	15884	L	337:00	81/362
SWP	16010	L	030:00	82/012
SWP	16431	L	450:00	82/061
SWP	16470	L	120:00	82/063
SWP	16471	L	050:00	82/063
SWP	16748	L	030:00	82/102
SWP	16843	L	030:00	82/118
SWP	16844	L	100:00	82/118
SWP	16845	L	075:00	82/118
SWP	16885	L	115:00	82/123
SWP	17680	L	340:00	82/228
SWP	17754	L	360:00	82/236
SWP	17838	L	030:00	82/246
SWP	17962	L	030:00	82/259
SWP	18334	L	045:00	82/293
SWP	18343	L	070:00	82/294
SWP	18841	L	240:00	82/355
SWP	19002	L	030:00	83/017
SWP	19169	L	040:00	83/062
SWP	19170	L	040:00	83/062
SWP	19171	L	040:00	83/062
SWP	19172	L	035:00	83/063
SWP	19178	L	080:00	83/338
SWP	19191	L	040:00	83/038
SWP	19196	L	060:00	83/038
SWP	19197	L	060:00	83/038
SWP	19434	L	290:00	83/077
SWP	19434	L	140:00	83/077
SWP	19443	L	230:00	83/074
SWP	19784	L	031:00	83/112
SWP	19814	L	030:00	83/117
SWP	19821	L	265:00	83/117
SWP	19845	L	030:00	83/119
SWP	20160	L	150:00	83/158
SWP	20196	L	120:00	83/164
SWP	20345	L	185:00	83/186
SWP	20354	L	325:00	83/187
SWP	20467	L	040:00	83/196
SWP	20471	L	030:00	83/199
SWP	20472	L	045:00	83/199
SWP	20661	H	300:00	83/224
SWP	21216	L	752:00	83/277
SWP	21263	L	135:00	83/284
SWP	21596	L	120:00	83/325
SWP	21696	L	120:00	83/341
SWP	21718	L	110:00	83/343
SWP	22778	L	180:00	84/109
SWP	22823	L	030:00	84/115
SWP	22870	L	090:00	84/121
SWP	23135	L	060:00	84/152
SWP	23687	L	820:00	84/229
SWP	25360	L	075:00	85/064
SWP	25515	L	070:00	85/084
SWP	25515	L	070:00	85/084
SWP	25517	L	120:00	85/085
SWP	25517	L	120:00	85/085
SWP	26149	H	107:00	85/163
SWP	26157	H	115:00	85/164
SWP	26619	H	210:00	85/230
SWP	26669	L	060:00	85/266
SWP	26699	L	060:00	85/267
SWP	26853	L	100:00	85/278
SWP	26854	L	130:00	85/278
SWP	27048	L	347:00	85/312
SWP	27435	L	235:00	86/005
SWP	29189	L	030:00	86/254
SWP	29383	L	170:00	86/280
SWP	29766	L	078:00	86/333
SWP	31027	L	210:00	87/144
SWP	31048	L	060:00	87/147
SWP	31053	H	120:00	87/147
SWP	31393	L	030:00	87/208
SWP	31398	L	060:00	87/208
SWP	31399	L	060:00	87/208
SWP	31527	L	120:00	87/222
SWP	31528	L	120:00	87/222
SWP	31529	L	120:00	87/223
SWP	31530	L	120:00	87/223
SWP	31531	L	090:00	87/223
SWP	31568	L	130:00	87/229
SWP	31919	L	300:00	87/268
SWP	32122	L	030:00	87/292
SWP	32125	L	030:00	87/293
SWP	34017	L	075:00	88/217
SWP	34029	L	120:00	88/221
SWP	34030	L	060:00	88/221
SWP	34031	L	050:00	88/222
SWP	34035	L	040:00	88/222
SWP	34046	L	040:00	88/221
SWP	34046	L	040:00	88/221
SWP	34286	H	038:00	88/272

TABLE 2

LWP Sky Background Images

	Image	Dsp	Time MIN:SC	Date YR/DAY		Image	Dsp	Time MIN:SC	Date YR/DAY
LWP	1349	L	715:00	81/245	LWP	3238	L	080:00	84/121
LWP	1350	L	360:00	81/244	LWP	5356	L	360:00	88/216
LWP	1351	L	220:00	81/244	LWP	5356	L	360:00	88/216
LWP	1375	L	766:00	81/324	LWP	5357	L	571:00	88/216
LWP	1555	L	095:00	82/146	LWP	5357	L	571:00	88/216
LWP	1650	L	270:00	82/239	LWP	6016	L	800:00	86/355
LWP	1681	H	345:00	82/273	LWP	6263	L	410:00	85/175
LWP	1884	H	220:00	83/152	LWP	6506	L	840:00	85/221
LWP	2022	L	150:00	83/294	LWP	7750	L	180:00	86/065
LWP	2339	L	175:00	83/335	LWP	9745	L	360:00	86/358
LWP	2347	L	440:00	83/338	LWP	10124	H	180:00	87/049
LWP	2348	L	275:00	83/338	LWP	10143	L	350:00	87/049
LWP	2350	L	537:00	83/338	LWP	10400	H	230:00	87/084
LWP	2354	L	120:00	83/341	LWP	10541	L	300:00	87/103
LWP	2364	L	070:00	83/343	LWP	10545	H	300:00	87/103
LWP	2369	L	700:00	83/343	LWP	10594	L	042:00	87/107
LWP	2536	H	360:00	84/004	LWP	11052	L	190:00	87/174
LWP	2728	H	440:00	84/034	LWP	11162	L	365:00	87/194
LWP	2830	L	300:00	84/055	LWP	11186	H	300:00	87/197
LWP	2980	L	060:00	84/079	LWP	11284	L	200:00	87/209
LWP	2981	L	040:00	84/079	LWP	11471	L	210:00	87/238
LWP	2982	L	035:00	84/079	LWP	12229	L	340:00	87/341
LWP	3164	H	268:00	84/109	LWP	12443	H	360:00	88/007

TABLE 3

LWR Sky Background Images

Image		Dsp	Time MIN:SC	Date YR/DAY	Image		Dsp	Time MIN:SC	Date YR/DAY
LWR	7631	L	140:00	80/120	LWR	13362	H	180:00	82/154
LWR	7656	L	135:00	80/125	LWR	13382	H	300:00	82/154
LWR	8156	L	145:00	80/183	LWR	13434	L	300:00	82/159
LWR	8381	L	776:00	80/211	LWR	13567	H	200:00	82/183
LWR	9128	L	290:00	80/298	LWR	13571	L	210:00	82/183
LWR	9382	L	234:00	80/330	LWR	13578	H	250:00	82/183
LWR	9393	L	410:00	80/334	LWR	13641	L	330:00	82/190
LWR	9401	L	286:00	80/334	LWR	13642	L	060:00	82/190
LWR	9467	L	360:00	80/345	LWR	13663	H	360:00	82/194
LWR	9490	L	382:00	80/349	LWR	13760	H	330:00	82/209
LWR	9502	L	389:00	80/351	LWR	13826	H	285:00	82/217
LWR	9616	L	505:00	81/003	LWR	14236	L	180:00	82/266
LWR	9871	L	420:00	81/038	LWR	14303	H	240:00	82/274
LWR	10007	H	120:00	81/056	LWR	14321	H	345:00	82/277
LWR	10008	H	120:00	81/056	LWR	14323	L	060:00	82/277
LWR	10074	L	570:00	81/065	LWR	14451	L	160:00	82/294
LWR	10134	L	370:00	81/073	LWR	14845	L	370:00	82/354
LWR	10492	L	250:00	81/122	LWR	14867	L	095:00	82/356
LWR	10503	L	345:00	81/123	LWR	15053	L	060:00	83/017
LWR	10522	L	367:00	81/125	LWR	15053	L	060:00	83/017
LWR	10682	L	190:00	81/143	LWR	15333	L	030:00	83/052
LWR	10711	L	050:00	81/148	LWR	15334	H	135:00	83/052
LWR	10713	L	120:00	81/148	LWR	15466	L	130:00	83/073
LWR	10714	L	110:00	81/148	LWR	15467	L	100:00	83/074
LWR	10949	L	360:00	81/177	LWR	15468	L	070:00	83/074
LWR	10961	L	235:00	81/179	LWR	15654	L	325:00	83/097
LWR	10965	L	150:00	81/180	LWR	16008	L	260:00	83/145
LWR	10980	L	200:00	81/183	LWR	16083	L	050:00	83/158
LWR	11224	L	400:00	81/215	LWR	16084	L	146:00	83/158
LWR	11267	L	250:00	81/221	LWR	16131	L	120:00	83/164
LWR	11447	H	030:00	81/243	LWR	16190	H	270:00	83/178
LWR	3799	L	300:00	79/050	LWR	16271	L	040:00	83/182
LWR	3913	L	360:00	79/066	LWR	16322	H	300:00	83/193
LWR	11841	L	120:00	81/299	LWR	16323	L	100:00	83/192
LWR	11844	L	040:00	81/299	LWR	16562	L	300:00	83/223
LWR	11881	L	340:00	81/306	LWR	16765	H	150:00	83/270
LWR	11925	L	205:00	81/310	LWR	16766	H	150:00	83/270
LWR	13026	L	455:00	82/106	LWR	16873	H	190:00	83/270
LWR	13027	H	120:00	82/106	LWR	16900	H	126:00	83/272
LWR	13031	L	390:00	82/107	LWR	17017	L	060:00	83/325
LWR	13040	L	250:00	82/108	LWR	17018	L	090:00	83/326
LWR	13188	L	040:00	89/040	LWR	17300	L	120:00	84/080
LWR	13224	H	240:00	82/132	LWR	17352	H	150:00	84/096
LWR	13323	H	180:00	82/147	LWR	17708	L	030:00	85/109
LWR	13327	L	210:00	82/148	LWR	17910	L	030:00	86/173
LWR	13336	H	300:00	82/152					

TABLE 4

TFLOOD Images - All Cameras

Images	Disp.	Time MIN:SC	Date YR/DAY
SWP 34678 - 34695	L	0:05	88/310
LWP 14501 - 14516	L	0:25	88/328
LWR 18271 - 18273	L	0:10	89/057
LWR 18275 - 18279	L	0:10	89/058
LWR 18284 - 18287	L	0:10	89/065

REFERENCES

Adelman, S.J. and Leckrone, D.S. 1985, *NASA IUE Newsletter*, **28**, 35.

Boggess, A. et al. 1978, *Nature*, **275**, 2.

Bohlin, R.C., Holm, A.V., Savage, B.D., Snijders, M.A.J., and Sparks, W.M. 1980, *Astr. Ap.*, **85**, 1.

Bruegman, O.W. and Crenshaw, D.M. 1989, *NASA IUE Newsletter*, **37**, 36.

Grady, C.A. and Imhoff, C.L. 1985, *NASA IUE Newsletter*, **28**, 86.

Hackney, K.R.H., Hackney, R. L., and Kondo, Y. 1985, *B.A.A.S.,* **16**, 904.

Hackney, K.R.H., Hackney, R. L., and Kondo, Y. 1984, *NASA CP*, **2238**, 335.

Linde, P. and Dravins, D. 1988, *NASA IUE Newsletter*, **36**, 18.

Nichols-Bohlin, J. 1988, *NASA IUE Newsletter.* **36**, 28.

Sonneborn, G., et al. 1987, *NASA IUE Newsletter* **32**, 1.

Turnrose, B.E. and Thompson, R.W. 1984. *IUE Image Processing Information Manual, Version 1.1*, CSC/TM-84/6058.

Turnrose, B.E., Harvel, C.A., and Stone, D.F. 1981, *IUE Image Processing Information Manual, Version 2.0*, CSC/TM-81/6268.

FIGURE CAPTIONS

Figure 1. SWP sky background spectra obtained in low- and high-dispersion modes, and SWP TFLOOD spectra obtained in low-dispersion mode. All data have been processed as both point-source and extended-source low-dispersion spectra. The spectra are given in time-integrated flux units (ergs cm^{-2} Å $^{-1}$) as a function of wavelength (Å). A horizontal line indicates the zero level for each spectrum.

Figure 2. SWP sky background spectra arranged in four chronological groups. The spectra are plotted as in Figure 1.

Figure 3. LWP sky background spectra obtained in low- and high-dispersion modes, and LWP TFLOOD spectra obtained in low-dispersion mode. Spectra over the wavelength range 2400Å to 3000Å are plotted as in Figure 1.

Figure 4. LWR sky background spectra obtained in low- and high-dispersion modes, and LWR TFLOOD spectra obtained in low-dispersion mode. Spectra over the wavelength range 2400Å to 3000Å are plotted as in Figure 1.

Figure 5. SWP sky background spectra processed as extended sources. The spectra were separated into groups according to exposure time and averaged; the average exposure time for each group is given. The spectra are given in time-integrated flux units over the wavelength range 1600Å to 2000Å .

Figure 6. The time-integrated flux of several artifacts have been averaged over small wavelength bins and plotted against exposure time (min). The straight lines are linear regression

fits for each artifact. The upper plots are for SWP extended- and point-source artifacts at the indicated wavelengths, and the lower plot is for an LWP point-source artifact at 2898Å and an LWR extended-source artifact at 3086Å .

Figure 7. SWP reference spectra showing camera artifacts in both point- and extended-source spectra. The spectra are averages of all sky backgrounds with exposure times between 180 and 440 min, and are given in flux units (ergs cm^{-2} Å $^{-1}$ sec^{-1}) as a function of wavelength (Å). A horizontal line indicates the zero level for each spectrum, and the presence of a reseau mark is indicated with an "R".

Figure 8. LWP reference spectra showing camera artifacts in both point- and extended-source spectra. The spectra are averages of all sky backgrounds with exposure times between 180 and 440 min, and are given in flux units (ergs cm^{-2} Å $^{-1}$ sec^{-1}) as a function of wavelength (Å). A horizontal line indicates the zero level for each spectrum, and the presence of a reseau mark is indicated with an "R".

Figure 9. LWR reference spectra showing camera artifacts in both point- and extended-source spectra. The spectra are averages of all sky backgrounds with exposure times between 180 and 440 min, and are given in flux units (ergs cm^{-2} Å $^{-1}$ sec^{-1}) as a function of wavelength (Å). A horizontal line indicates the zero level for each spectrum, and the presence of a reseau mark is indicated with an "R". The hot spot is indicated with an "H".

Principal Author's Address

D. Michael Crenshaw
Astronomy Programs
Computer Sciences Corporation
10000A Aerospace Road
Lanham-Seabrook, MD 20706
electronic mail: SPAN network - IUEGTC::CRENSHAW

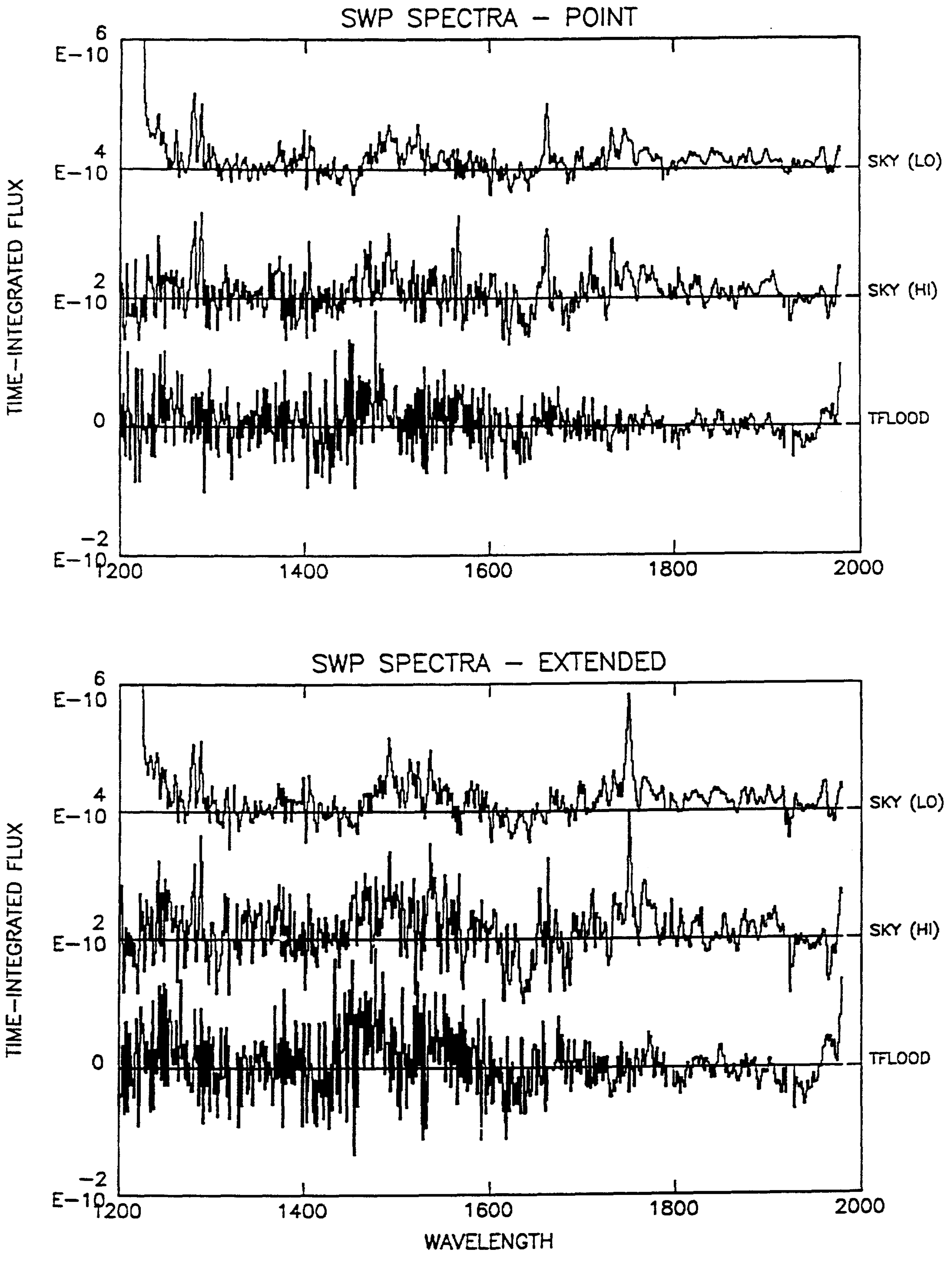
SWP SPECTRA - POINT
6 E-10
4 E-10
2 E-10
0
-2 E-10
TIME-INTEGRATED FLUX
1200
1400
1600
1800
2000
SKY (LO)
SKY (HI)
TFLOOD
SWP SPECTRA - EXTENDED
WAVELENGTH

Fig. 1

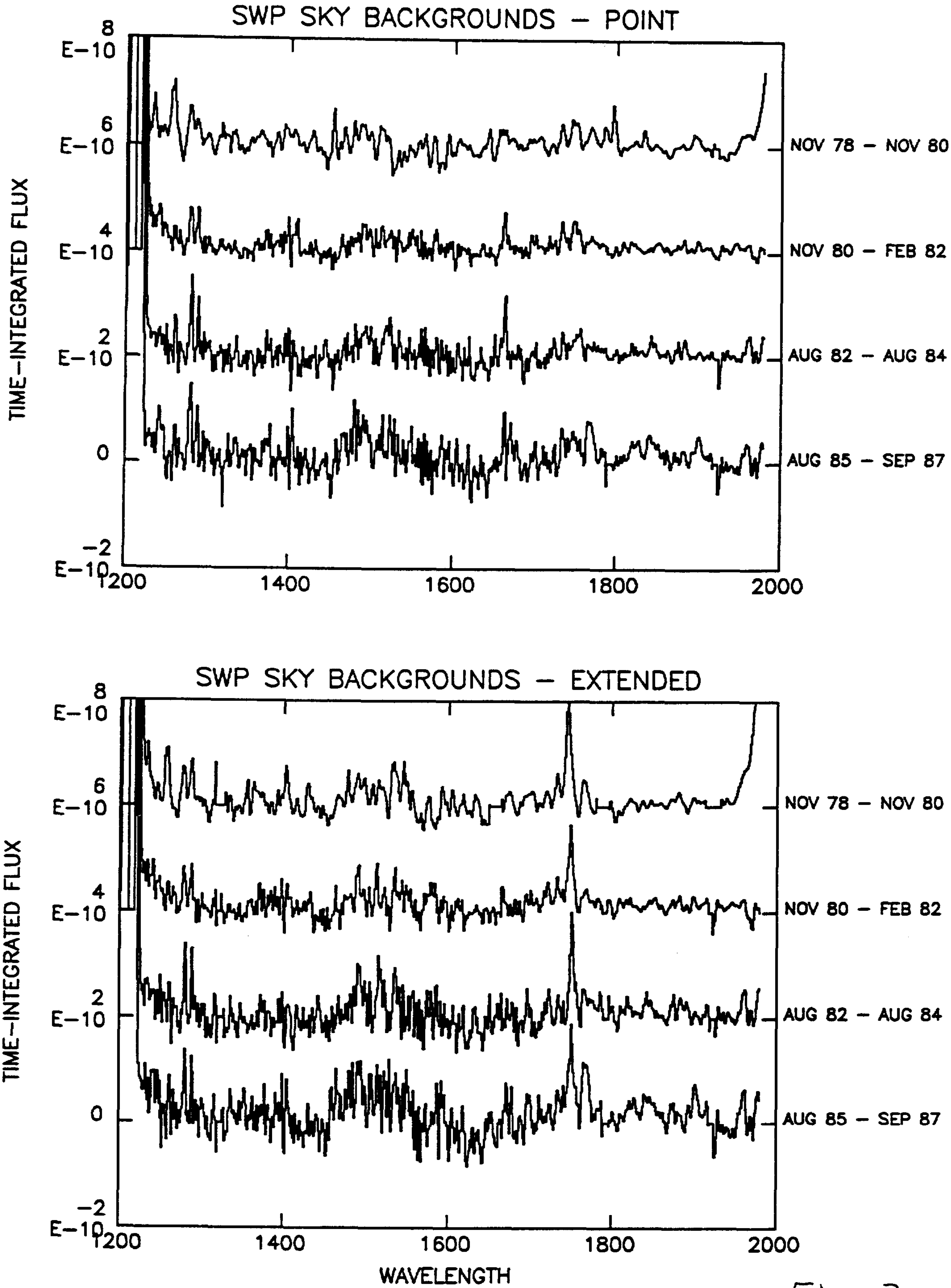

SWP SKY BACKGROUNDS – POINT
TIME-INTEGRATED FLUX
8 E-10
6 E-10
4 E-10
2 E-10
0
-2 E-10
1200
1400
1600
1800
2000
NOV 78 – NOV 80
NOV 80 – FEB 82
AUG 82 – AUG 84
AUG 85 – SEP 87
SWP SKY BACKGROUNDS – EXTENDED
TIME-INTEGRATED FLUX
WAVELENGTH

Fig. 2

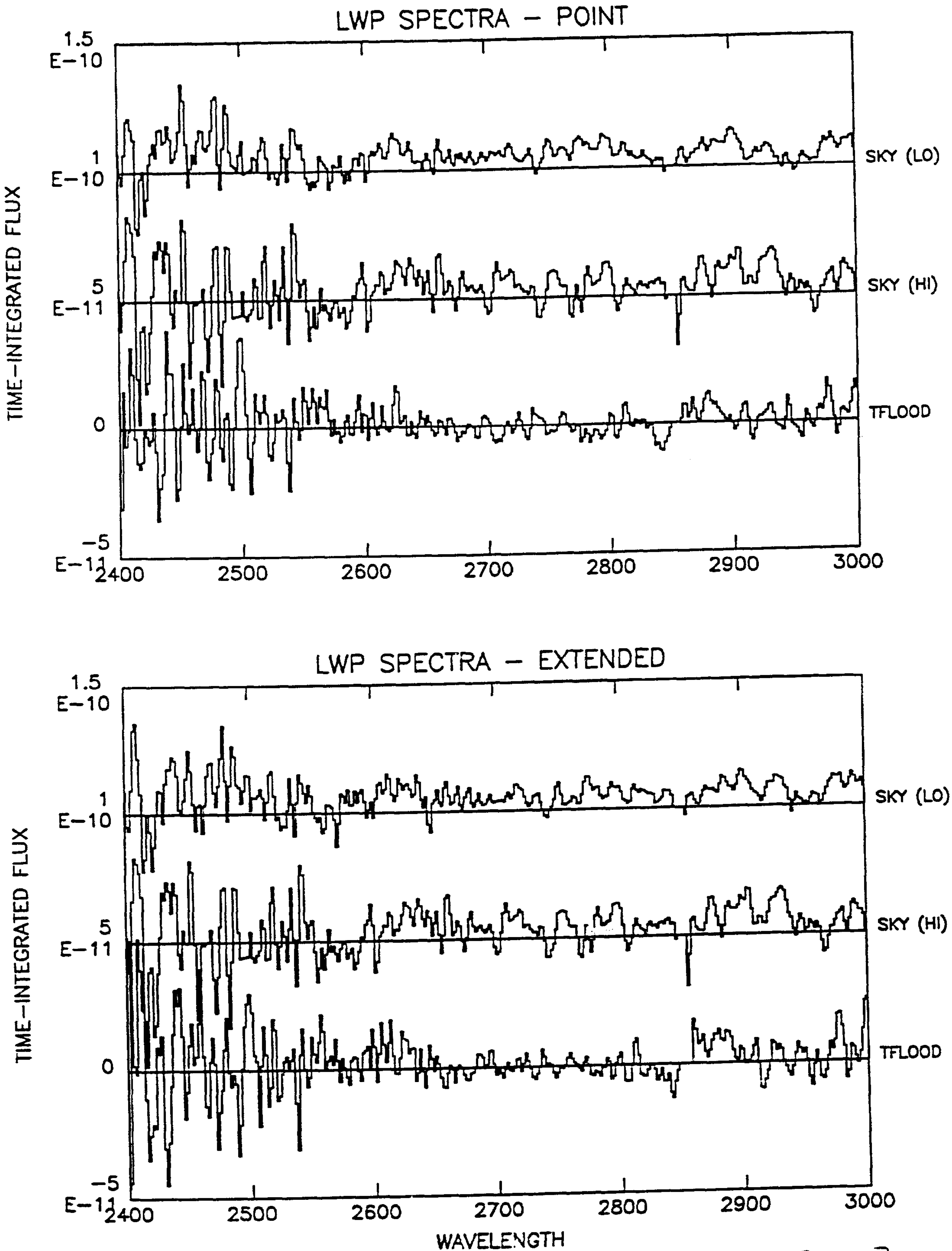
LWP SPECTRA – POINT
1.5 E–10
1 E–10
5 E–11
0
–5 E–11
TIME–INTEGRATED FLUX
SKY (LO)
SKY (HI)
TFLOOD
2400
2500
2600
2700
2800
2900
3000
LWP SPECTRA – EXTENDED
1.5 E–10
1 E–10
5 E–11
0
–5 E–11
TIME–INTEGRATED FLUX
SKY (LO)
SKY (HI)
TFLOOD
2400
2500
2600
2700
2800
2900
3000
WAVELENGTH

Fig. 3

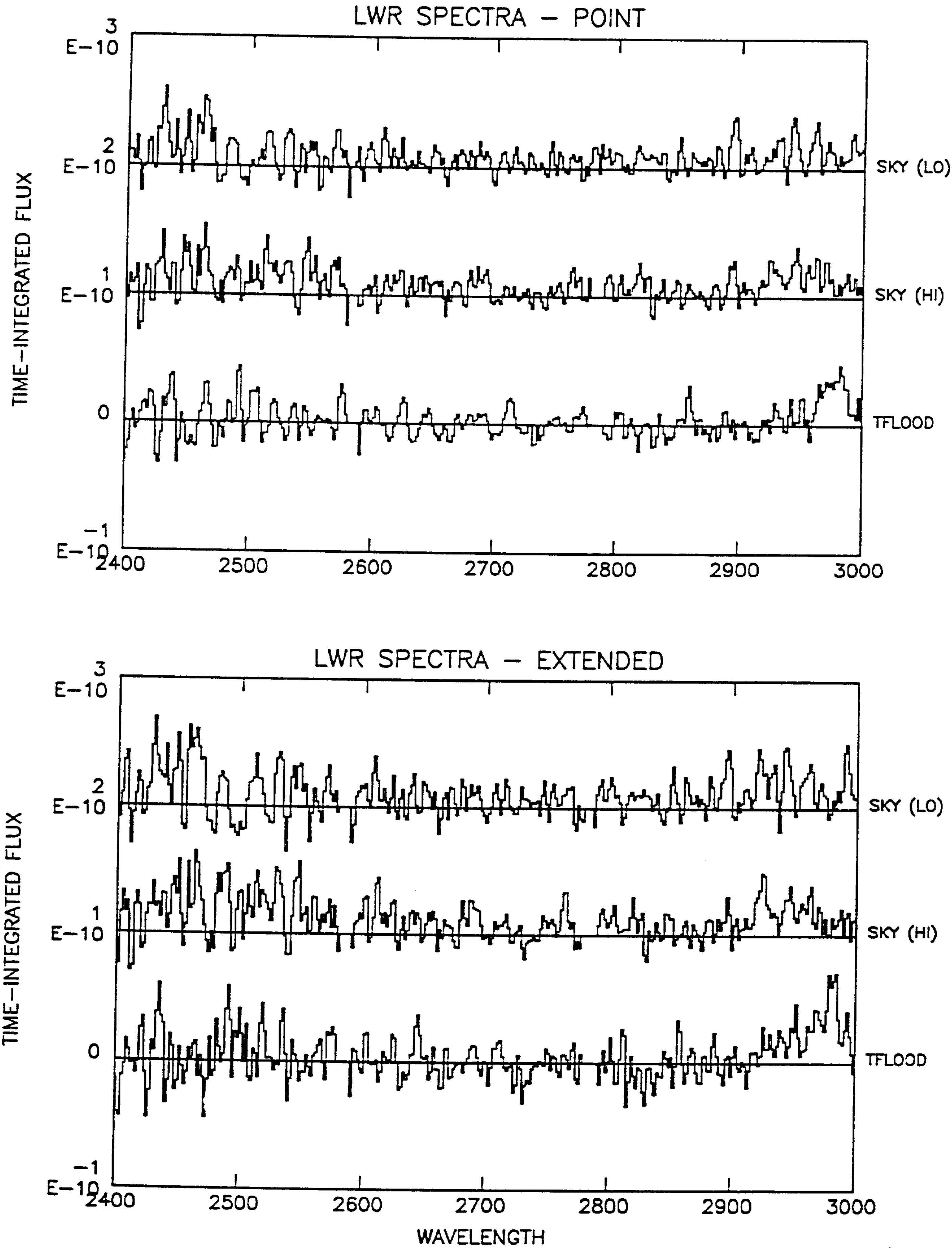
LWR SPECTRA - POINT
TIME-INTEGRATED FLUX
3 E-10
2 E-10
1 E-10
0
-1 E-10
2400
2500
2600
2700
2800
2900
3000
SKY (LO)
SKY (HI)
TFLOOD
LWR SPECTRA - EXTENDED
TIME-INTEGRATED FLUX
3 E-10
2 E-10
1 E-10
0
-1 E-10
2400
2500
2600
2700
2800
2900
3000
WAVELENGTH
SKY (LO)
SKY (HI)
TFLOOD

Fig. 4

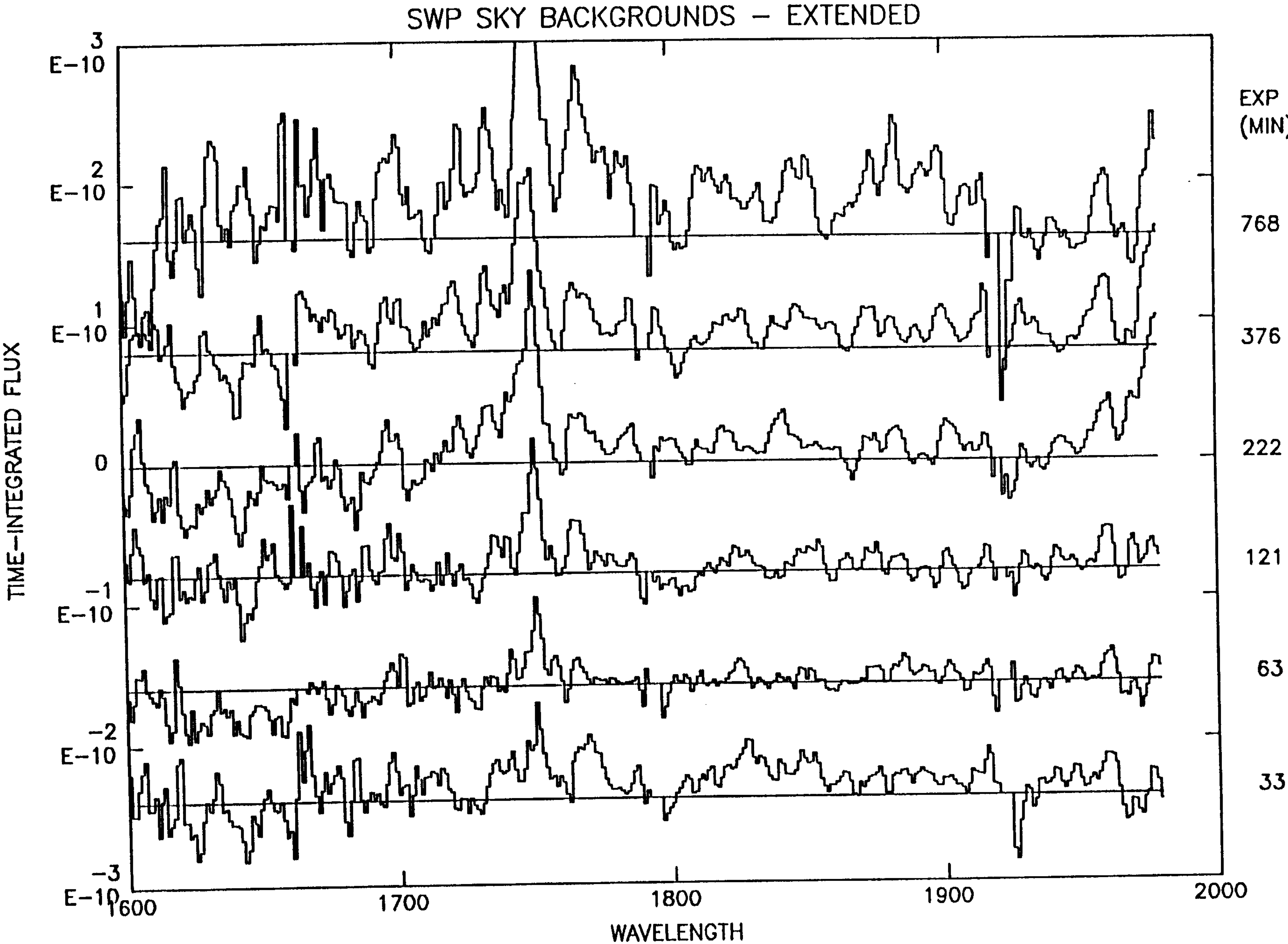

203

Fig. 5

Fig. 5

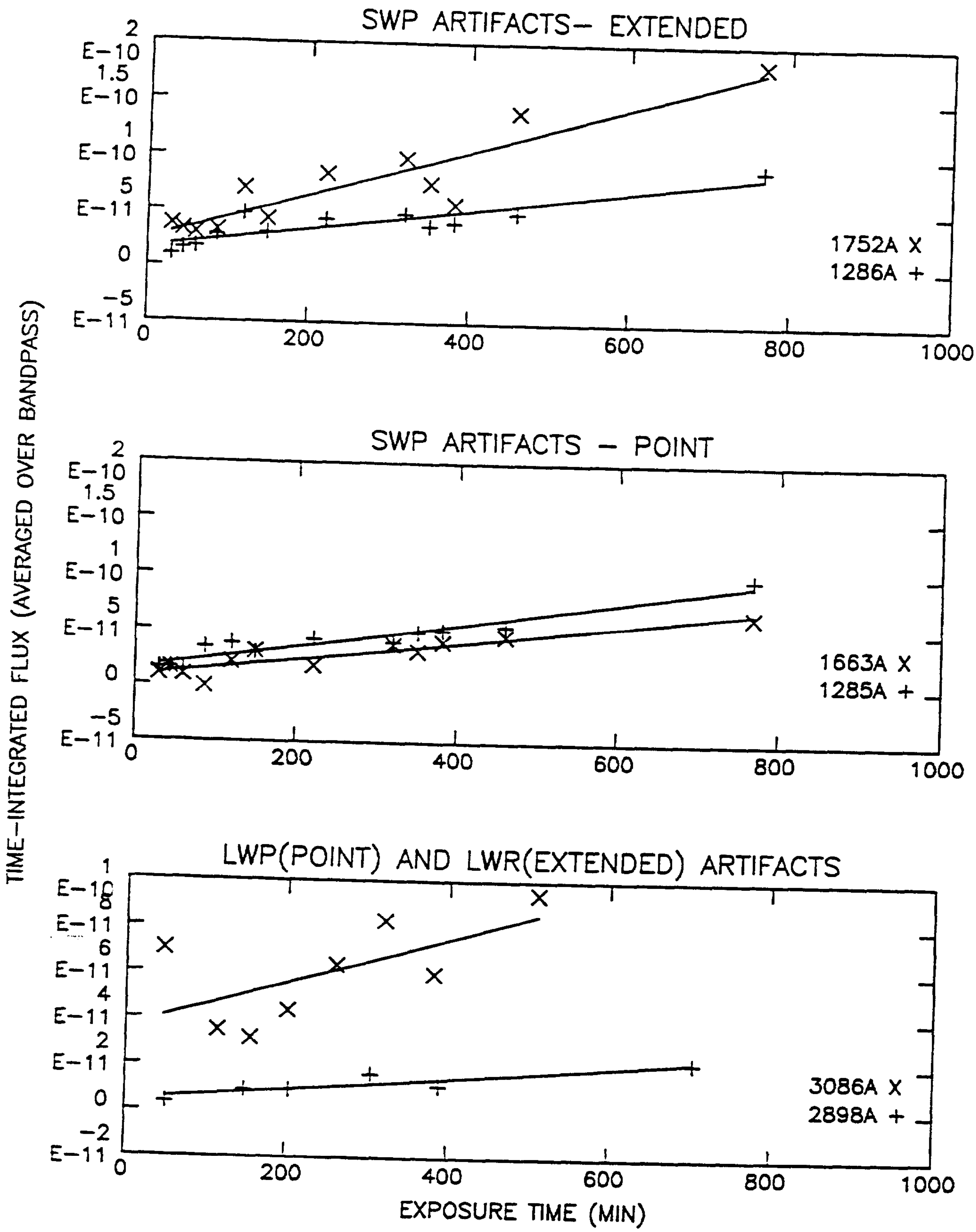

SWP ARTIFACTS— EXTENDED
1752A X
1286A +
SWP ARTIFACTS – POINT
1663A X
1285A +
LWP(POINT) AND LWR(EXTENDED) ARTIFACTS
3086A X
2898A +
TIME-INTEGRATED FLUX (AVERAGED OVER BANDPASS)
EXPOSURE TIME (MIN)

Fig. 6

SWP REFERENCE ARTIFACT SPECTRA

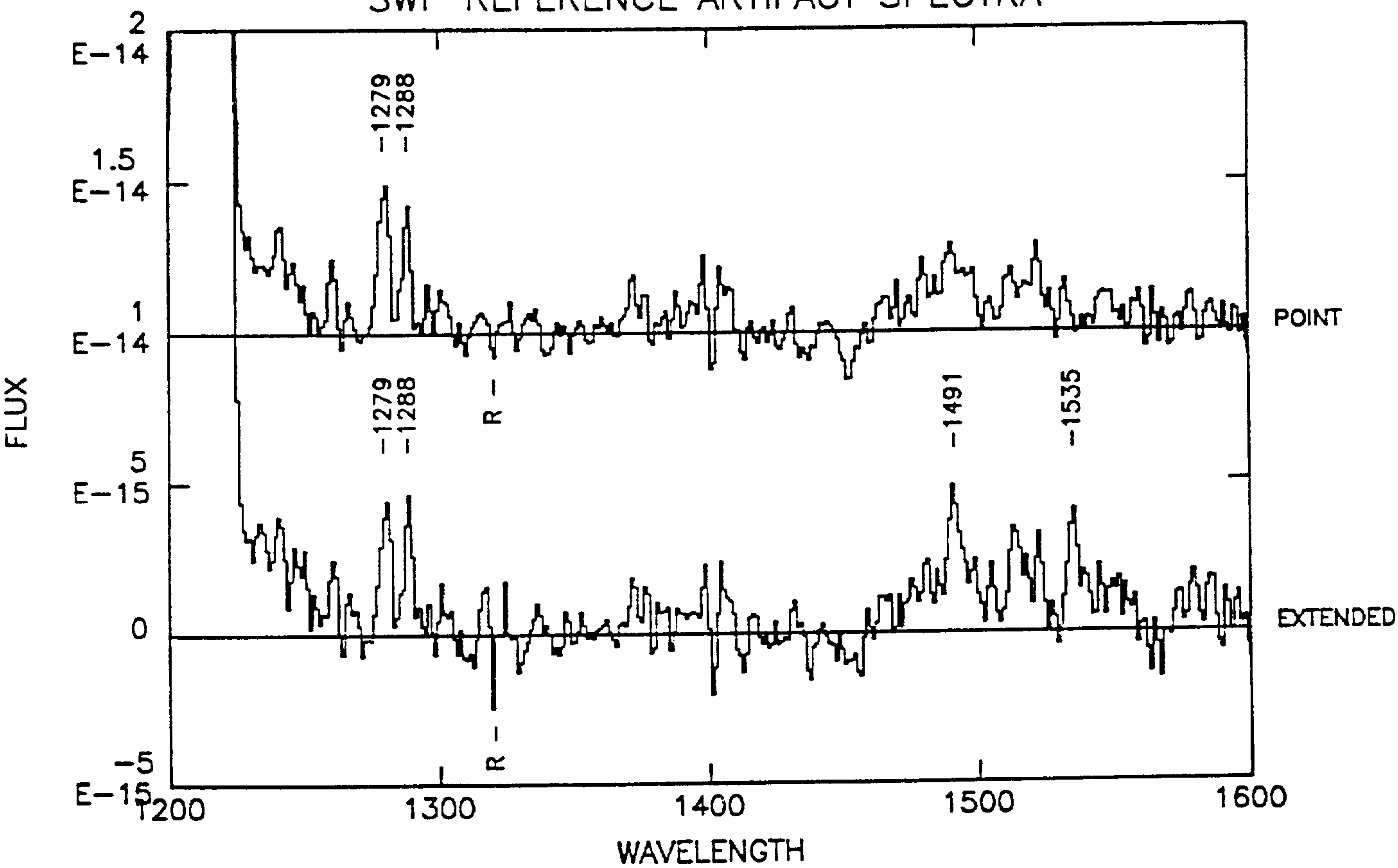

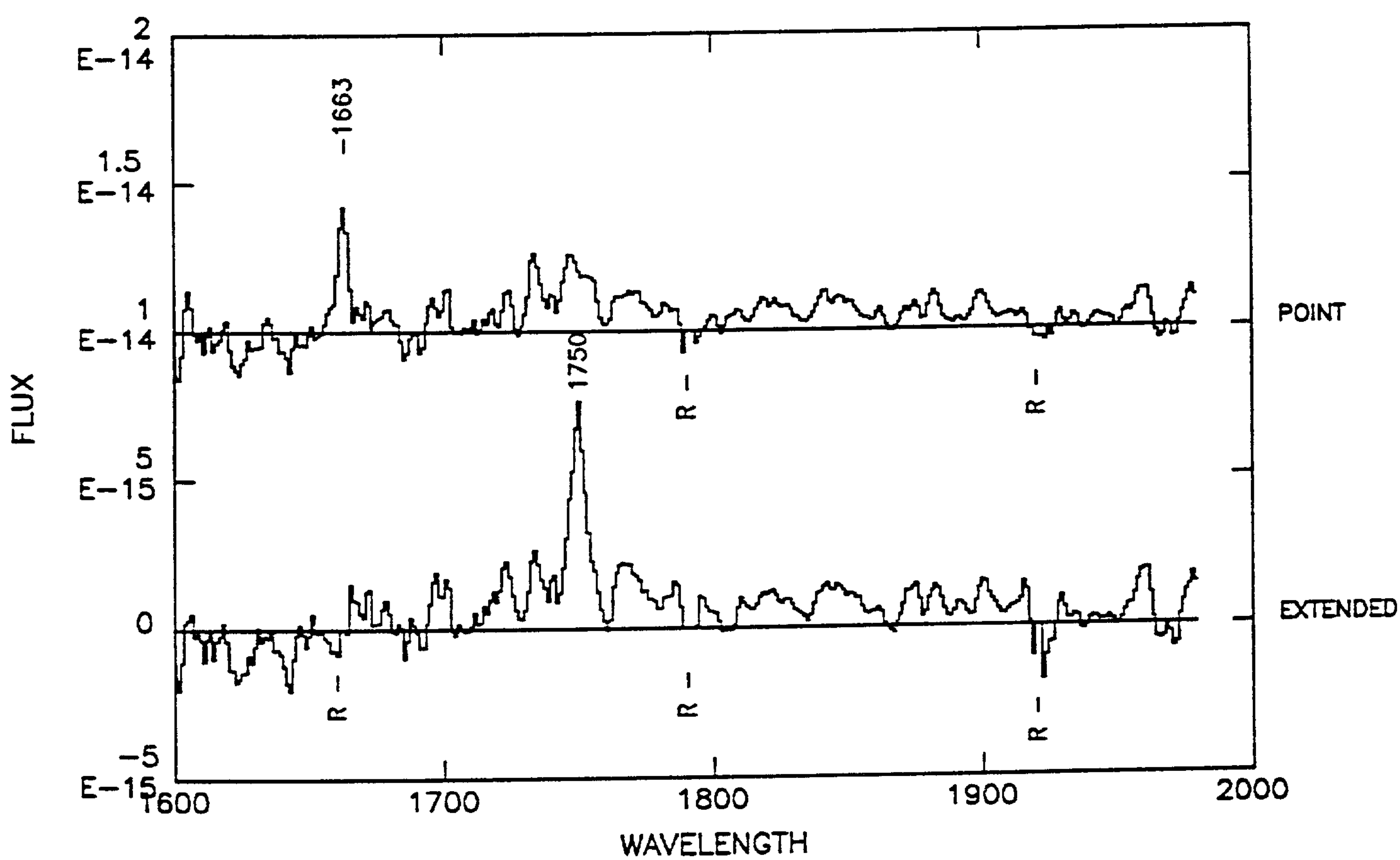

Fig. 7

LWP REFERENCE ARTIFACT SPECTRA

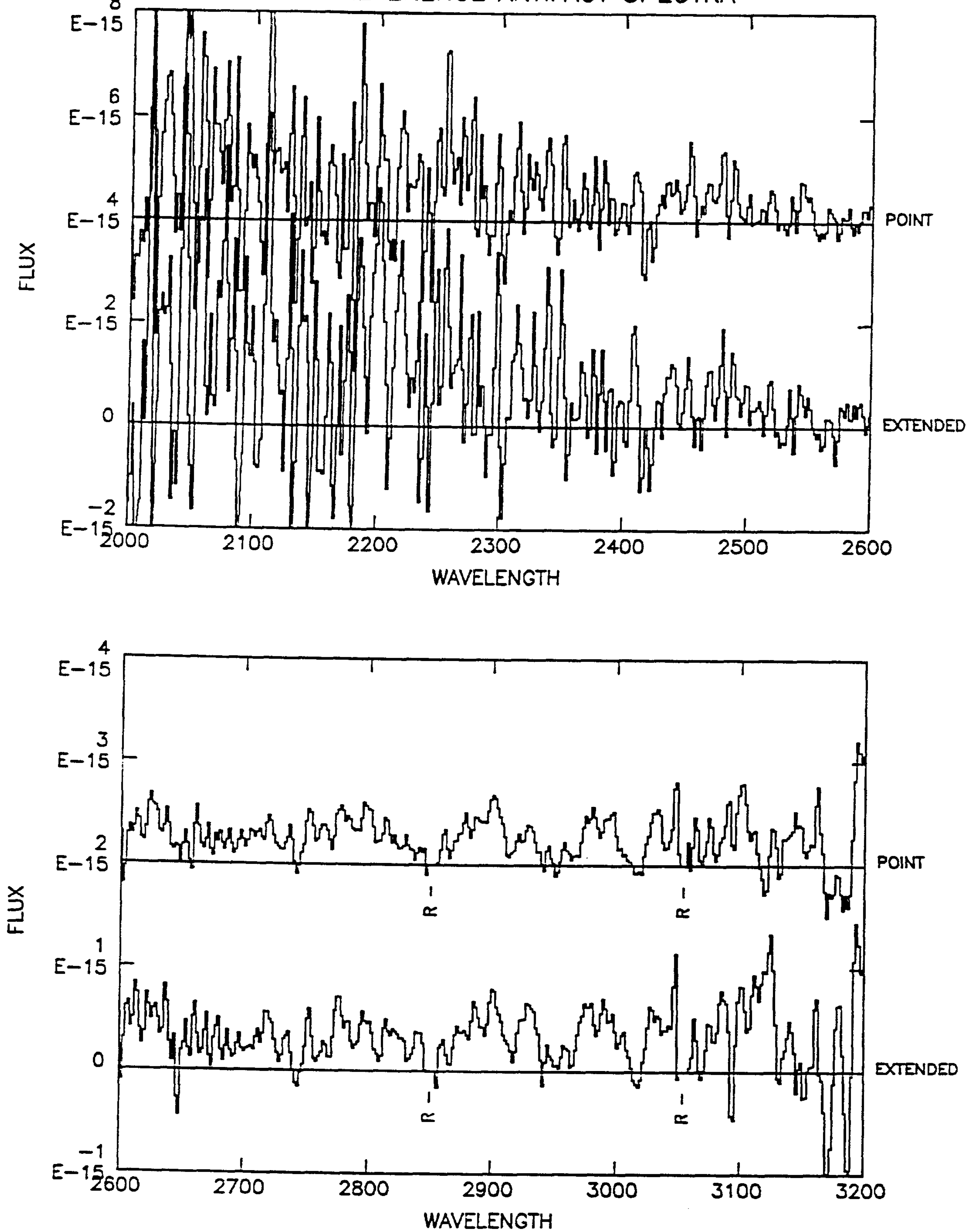

Fig. 8

LWR REFERENCE ARTIFACT SPECTRA

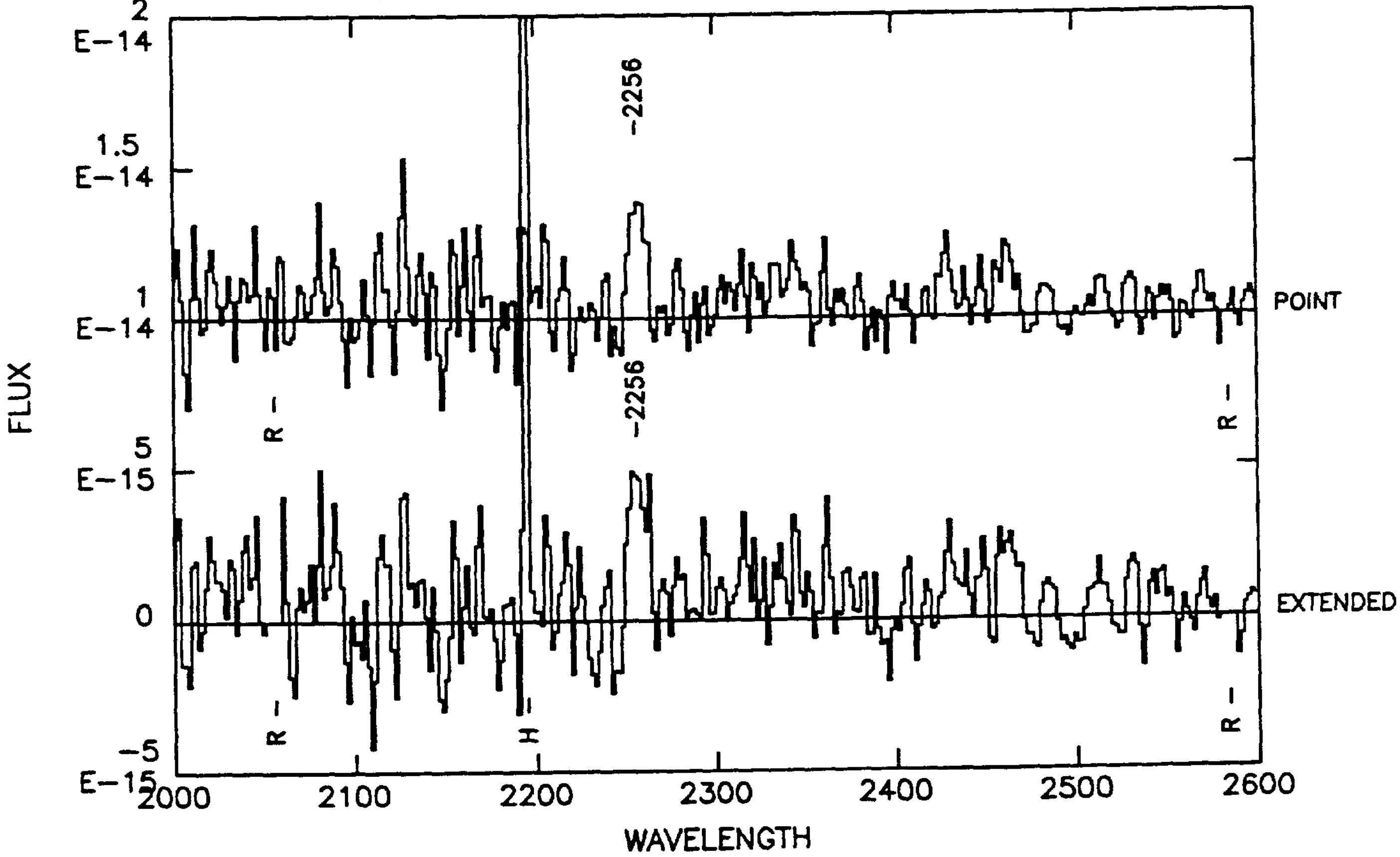

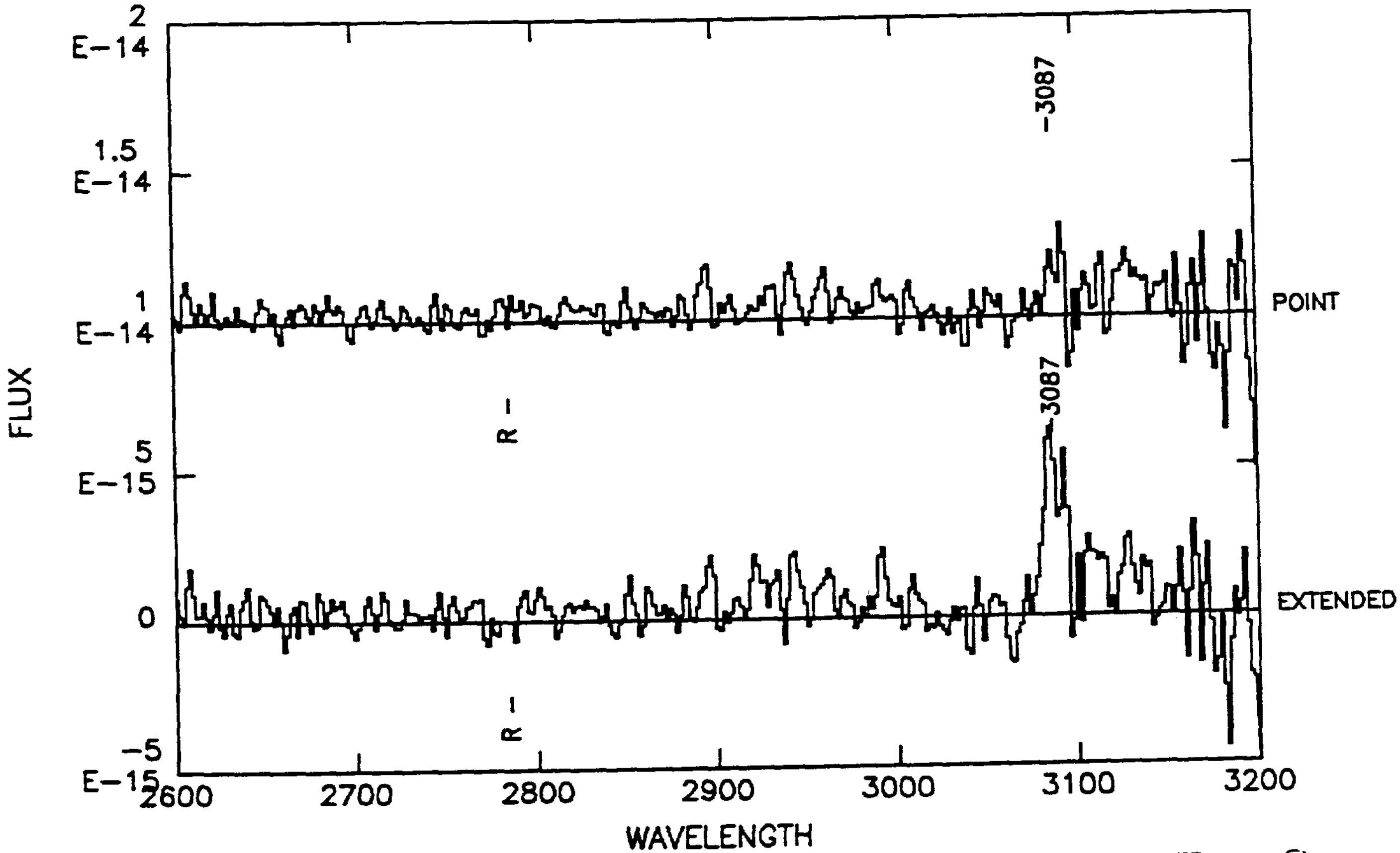

Fig. 9